24th COBEM - 2017

24th ABCM International Congress of Mechanical Engineering
December 3-8, 2017, Curitiba, PR, Brazil

# COBEM-2017-0958
# INFLUENCE OF GEOMETRIC PARAMETERS IN THERMAL BEHAVIOR OF THE RECEIVER OF A LINEAR FRESNEL REFLECTOR SYSTEM

**Patricia Scalco**
*Mechanical Engineering Graduate Program - Universidade do Vale do Rio dos Sinos, Av. Unisinos, 950, Bairro Cristo Rei, CEP: 93.022-750*
*patrscalco@edu.unisinos.br*

**Jacqueline Copetti**
*Mechanical Engineering Graduate Program - Universidade do Vale do Rio dos Sinos, Av. Unisinos, 950, Bairro Cristo Rei, CEP: 93.022-750*
*jcopetti@unisinos.br*

**Mario Henrique Macagnan**
*Mechanical Engineering Graduate Program - Universidade do Vale do Rio dos Sinos, Av. Unisinos, 950, Bairro Cristo Rei, CEP: 93.022-750*
*mhmac@unisinos.br*

***Abstract.*** *The use of Linear Fresnel Reflectors (LFR) appears as an alternative in the application of Concentrated Solar Power (CSP) for systems that need working fluids temperatures above 150 °C. Thus, the study of receptor, where the conversion of Direct Normal Irradiation (DNI) occurs, becomes important. The secondary concentrator consists of a reflective surface and allows maximizing the amount of rays absorbed by the receiver. Its geometry varies and depends on the demands of the studied system. For this work, a CPC (Compound Parabolic Collector) secondary concentrator type and one absorber tube configuration were used. The purpose of this study was analyze the influence of the geometric parameters on the thermal performance of the LFR arrangement receiver. For this, a thermal balance analysis was made considering the radiative effects of the three surfaces involved in this process (absorber tube, secondary concentrator surface and glass plate). Thus, it was possible to establish a relationship between the length of the absorber tube, and the thermal losses and efficiency of the system. In the geometric analysis, the interception factor was was 44 % for the system without the glass plate and 56 % for the isolated system (with the glass plate). Through the thermal analysis, it was defined the efficiency of the system, that for the best working condition was about 80%*

***Keywords:*** *Linear Fresnel Reflector, Concentrated Solar Power, Secondary Concentrator, Thermal Balance, Geometric Parameters.*

## 1. INTRODUCTION

The sun's energy is currently used as power source for photovoltaic systems, heating systems or concentrated solar power systems (CSP). The main solar concentration technologies are: Parabolic Trough Collector (PTC), Parabolic Dish Reflector (PDR), Heliostat Field Collector (HFC), and Linear Fresnel Reflector (LFR). The latter, the focus of this paper, transfers energy from the Sun to a working fluid (also called a heat exchange fluid or FTC).

In general, CSP plants that use LFR (Figure 1), are composed by rows of mirrors that move along the day following the Sun's path, receive normal direct irradiation (DNI) and reflect it to the receiving element. The receiver is composed by three parts: (1) the absorber tube, where an FTC flows; (2) a second reflective surface, called secondary concentrator, which has the function of maximizing the amount of rays that are absorbed by the absorber tube. The most used geometries for the secondary concentrator are trapezoidal and CPC; (3) a glass plate that has the purpose of minimizing the heat losses of absorber by convection and radiation.

The secondary concentrator has been object of many studies. The format of the secondary concentrator influences directly the performance of the arrangement. Lai *et al.* (2013), Moghimi *et al.* (2014), Natarajan *et al.* (2012) and Sahoo *et al.* (2012) presented results for studies using trapezoidal secondary concentrators. Heimsath *et al.* (2014) and Hoffer *et al.* (2015) show researches applying a secondary concentrator of CPC format. Qiu *et al.* (2015), presents a numerical analysis both for optical and thermal parameters. In this case, it was used an open receiver, i.e., the receiver assembly

without the glass plate. The results found for this analysis was 55 % for optical efficiency and 70 % for thermal efficiency. Balaji *et al.* (2016), shows an experimental study for a LFR system with an area of 154 m². The receiver is composed by a CPC secondary concentrator surface, one absorber tube and a glass plate. The optical efficiency was 63,2 % and the statistical tool used for the ray tracing analysis was the MonteCarlo, the same of the present paper.

Based on these studies, it is evident that the optimization of the geometric parameters to achieve a satisfactory thermal performance is justified. For the present study, a receiver with CPC format for the secondary concentrator, absorber tube and glass enclosure was used. The condition of the receptor isolated was considered. Therminol VP1 was used as thermal exchange fluid. This theoretical study was developed using the softwares MATLAB and EES.

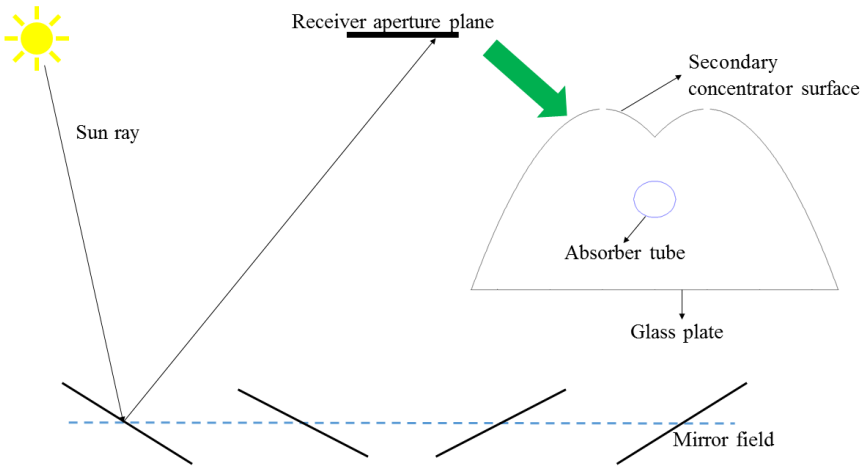


Figure 1. Representation of LFR system with a CPC secondary concentrator type.

First, the geometric analysis will be presented. It was studied CPC because its good optical performance and better concentration factor, due to its parabolic format, according to studies carried by Abbas *et al.* (2012) and Walker (2013). Initially, the ray tracing was carried out with the purpose of evaluating behavior of the rays upon reaching the receiving element. From this, a comparative analyzes were made between the two geometries. The following parameters were compared: diameter and the position of absorber tube inserted inside the secondary concentrator.

The second step was the analysis of the thermal behavior of the receiver. Thermal balances were developed to evaluate conductive, convective and radiative effects. With this, it was possible to define the rate of absorbed heat and heat loss, consequently, the thermal efficiency of the receiver for different working conditions. The influence of the mass flow rate, the tube length of the inlet fluid temperature and the DNI incident on the thermal performance of the receiver were evaluated.

## 2. GEOMETRICAL ANALYSIS OF THE RECEIVER

For the geometrical analysis of the receiver it was used previous results from a study by Muller (2016), which established the geometric parameters of the mirror field (number, width and length of the mirrors, as well as the spacing between them), height of the receiver and opening of the secondary concentrator, in addition to the power data arriving at the receiver over the period of one year. With these results was carried out the study of the secondary concentrator geometry and the ray tracing for the receiver with the secondary concentrator of format CPC.

Initially, the method of Mont Carlo (MMC) was applied, which allowed to evaluate the effect of the position of the absorber tube inside the receiving cavity. The study was carried out for two situations: first with the secondary concentrator without glass, where the rays originated from a hypothetical plane located in the opening of the concentrator and with a transparent glass plate inserted in the bottom, whose objective is to minimize thermal losses to the environment.

Sampling of random points was distributed within the range comprising the opening of the secondary concentrator. From each of the random points, a ray was generated, called incident ray. For each ray, a random angle was generated within the range of the acceptance angle. The maximum acceptance angle was initially calculated so the incident ray on the receiver converges and the interactions required to reach the absorber tube or the wall of the concentrator secondary occur.

The incident ray suffers multiple reflections inside the receiver until it reaches the absorber tube or until it is lost to the ambiance. Within this analysis, there are several possible scenarios: (1°) the incident ray reaches the absorber tube, being added to the absorbed flow; (2°) the ray strikes one of the walls of the secondary concentrator. In this case, it is

verified what point of the wall the ray stroked and a new ray is generated from that point (with the same angle of the incident ray, according to the reflection principle of Snell-Descartes). And again, it is verified where the ray stroked: if the ray stroked the absorber tube, it is added to the absorbed flow; if the ray stroked one of the walls of the secondary concentrator, the above procedure is repeated until it strikes the absorber tube and; (3°) the ray falls one or more times on the walls of the secondary concentrator and ends up being thrown out of the secondary concentrator, in this situation, the radius is added to the lost flux. The flowchart used for programming is shown in Figure 2.

The ray tracing allows evaluating the interception factor in the receiver. For the definition of the interception factor some geometric parameters are taken in account, like the height of the absorber, the aperture area of the absorber and the position of the absorber tube inside the receiver cavity. It is important to highlight that the secondary concentrator must be built by materials with a good reflectivity, so the incident may reflect more than one time inside the receiver before to be added to the absorber flux. Instead, the absorber tube must consist of a material with good absorptivity.

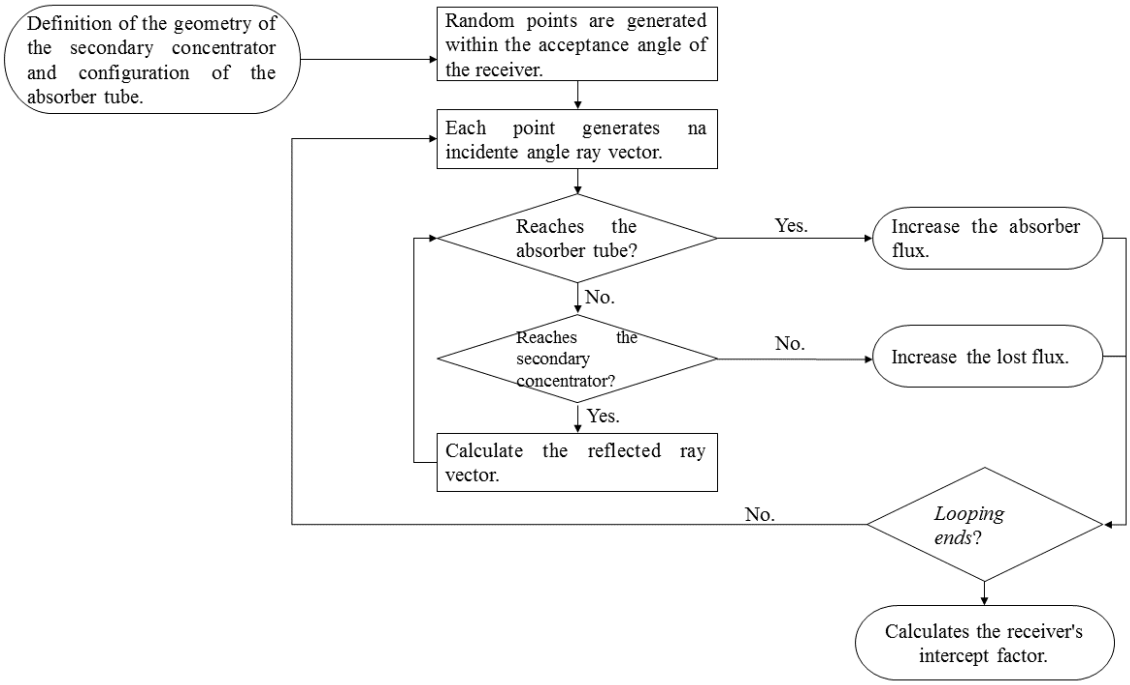


Figure 2. Routine developed in MATLAB for ray tracing and analysis of the interception factor in the secondary concentrator.

With the definition of the ray tracing, it is possible to determine the interception factor, $\eta_{if}$. The interception factor represents the fraction of rays that reaches the absorber tube and it is given by the Eq. 1:

$$\eta_{fi} = \frac{Q_a}{Q} \tag{1}$$

where $Q_a$ represents the amount of rays that reaches the absorber tube and Q represents the total amount of incident rays in the receiver.

## 3. THERMAL ANALISYS OF THE RECEIVER

The second part of the paper was the analysis of thermal behavior of the receiver of LFR system. For this stage, the interception factor is used to define the thermal performance of the receiver. It was verified how much of the incident radiation is converted, in fact, into useful heat, besides verifying the thermal losses. As mentioned above, the software EES was used as a calculation tool and the receiver was imposed the condition of isolated concentrator of CPC format, with an absorber tube and glass plate.

Thermal balances were performed on different surfaces and the effects of conduction, convection and radiation were considered. From this, the heat rate converted to useful heat for the system and the heat rate loss were defined. The thermal efficiency of the receiver is also determined for many conditions of operation.

In the absorber tube, the balances for the inner and outer walls are described from Eq. (2) and Eq. (3), respectively:

$$q_{cond\ t} = q_{convi\ t} \tag{2}$$

$$q_{abs\ t} = q_{cond\ t} + q_{conve\ t} + q_{rad\ ts} + q_{rad\ tg} \tag{3}$$

where $q$ means the rate of heat transferred and the index that follows it indicates how this transfer takes place: *cond* represents the transfer by conduction; *conv*, convection; *rad* the radiation and; *abs* is the rate of heat absorbed. Besides these indices, it is possible to identify in which part of the receiver it happens by observing the subscripts: *t*, tube; and, envelope; *g*, glass; *s*, secondary concentrator surface.

The thermal balance in the glass plate are given by Eq. (4) and Eq. (5):

$$q_{convi\ g} + q_{rad\ tg} + q_{rad\ sg} = q_{cond\ g} \tag{4}$$

$$q_{abs\ g} + q_{cond\ g} = q_{conve\ g} + q_{rad\ gm} \tag{5}$$

where the subscript m represents the mirror field.

The balance on the inner surface of the secondary concentrator is given by Eq. (6):

$$q_{abs\ s} + q_{rad\ ts} + q_{conv\ s} = q_{cond\ s} + q_{rad\ sv} \tag{6}$$

The thermal losses of the system consider the losses by convection and radiation to the external environment and the loss by conduction through the wall of the secondary concentrator, according to Eq. (7).

$$q_{losses} = q_{conve\ g} + q_{rad\ gm} + q_{cond\ s} \tag{7}$$

The useful heat is given by:

$$q_{useful} = q_{convi\ t} = \dot{m} c_p (T_{in} - T_{out}) \tag{8}$$

where $\dot{m}$ is the mass flow rate; $c_p$ the specific heat of the working fluid; $T_{in}$ and $T_{out}$ are the inlet and outlet temperatures, respectively. In Figure 3, it is possible to observe a representation of the heat transfer rates at the receiver. The arrows in blue represent the heat rates absorbed by the system, while the arrows in red represent the thermal losses.

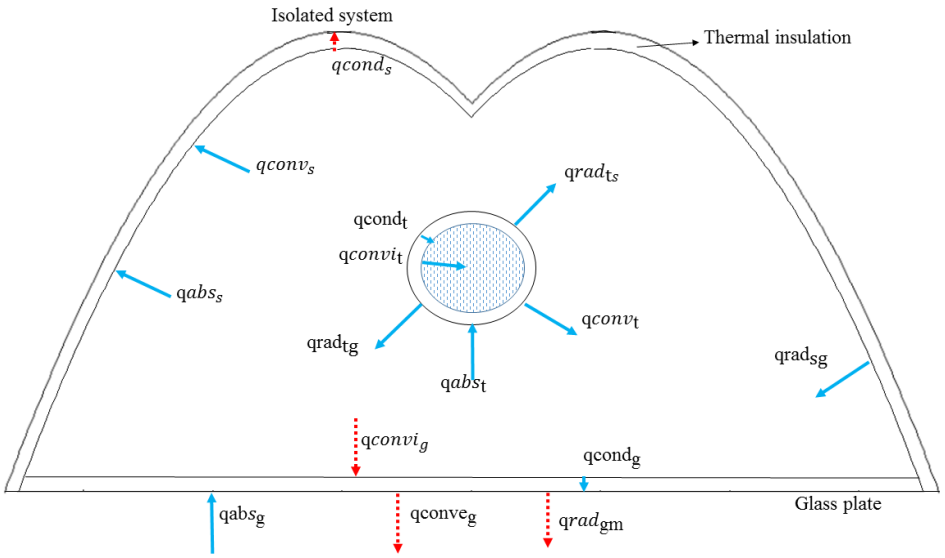


Figure 3. Representation of the heat transfer rates in the receiver.

For radiation, the radiative energies of each of the surfaces were considered, for this it is necessary to know the view factors. The view factor was determined from the geometric relation between the surfaces involved in the thermal exchange. The following relationships were considered: $F_{ts}$ and $F_{st}$ (view factor of the absorber tube in relation to the secondary concentrator surface and the reverse, by the reciprocal relationship), $F_{tg}$ (absorber tube view factor in relation to the glass plate), $F_{sg}$ and $F_{gs}$ (secondary concentrator view factor in relation to the glass plate and the reverse) and $F_{gm}$ (view factor of the glass plate in relation to the field of mirrors).

$$F_{ts} = \frac{\pi D}{P}\left(1 - \frac{1}{\pi} tan^{-1}\frac{w_g}{a}\right) \tag{9}$$

where $D$ is the diameter of the absorber tube; $P$ is the perimeter of the secondary concentrator; $w_g$ represents the width of the glass plate and $a$ is the height of the absorber tube relative to the base of the secondary concentrator.

$$F_{st} A_S = F_{ts} A \tag{10}$$

where $A_S$ is the surface area of the secondary concentrator and $A$ the area of the absorber tube. To define the view factor between the tube and the glass, the relation of Modest (2003) represented by Eq. (11) were used:

$$F_{tg} = \frac{1}{\pi}\left(tan^{-1}\frac{w_g}{a}\right) \tag{11}$$

As already mentioned, the view factor is a geometric relation between the surfaces, so it can be concluded that the form factor between the envelope and the glass is obtained through Eq. (12):

$$F_{sg} = 1 - F_{st} \tag{12}$$

and $F_{gs}$ by the relation of reciprocity.

$$F_{sg} A_S = F_{gs} A_g \tag{13}$$

where $A_g$ is the area of the glass plate. The view factor between the glass and the field of mirrors, $F_{gm}$, also needs to be considered to obtain a closer analysis of the real. The view factor for this geometry was established by Wong (1976) and is given by Eq. (14):

$$F_{g,m} = \frac{H}{2w}\left[\sqrt{\left(\frac{w_g}{H} + \frac{w_m}{H}\right)^2 + 4} - \sqrt{\left(\frac{w_m}{H} - \frac{w_g}{H}\right)^2 + 4}\right] \tag{14}$$

where $H$ is the height of the receiver in relation to the mirrors field and $w_m$ is the width.

## 4. RESULTS AND DISCUSSION

The study developed by Muller (2016) provided the data about the mirror field. For the study, a field with 14 rows of mirrors, each one 300 mm wide and spaced 10 mm between each row. The receiver is positioned 3 m high in relation to the mirrors and it has a width of 350 mm. The mirrors used have a reflectivity of 0.94. For this configuration, the solar power arriving in the plane of the receiver is approximately 21 kW/m.

For the geometric analysis, two different situations were analyzed. First, the receiver with the absorber tube and the secondary concentrator surface. The second analysis was made with the insertion of a glass plate. It were analyzed the effects of refraction and reflection caused by the glass plate and its influence on the interception factor.

Figure 4 shows the relationship between height of absorber tube inside the receiver cavity and interception factor for concentrator with and without glass.

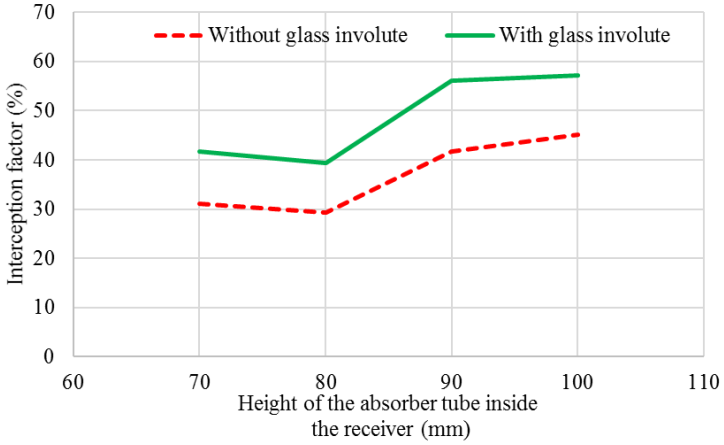


Figure 4. Height of the absorber tube inside the receiver cavity vs. Interception factor whit and whitout the glass plate.

The thermal analysis was developed for a stainless-steel absorber tube of 50 mm of diameter, positioned 90 mm from the receiver base, which contains a glass plate with a thickness of 5 mm; secondary concentrator of type CPC with external insulation of rock wool with thickness of 10 mm. For this geometric configuration, the intercept factor is 57%.

Initially, the influence of mass flow rate on thermal efficiency was verified. Figure 5 shows the relation between the efficiency (η) and tube length (L) for different fluid mass flow rates. The variations of fluid temperature between the inlet and outlet of the absorber tube and its length for different mass flow rate are presented in Figure 6.

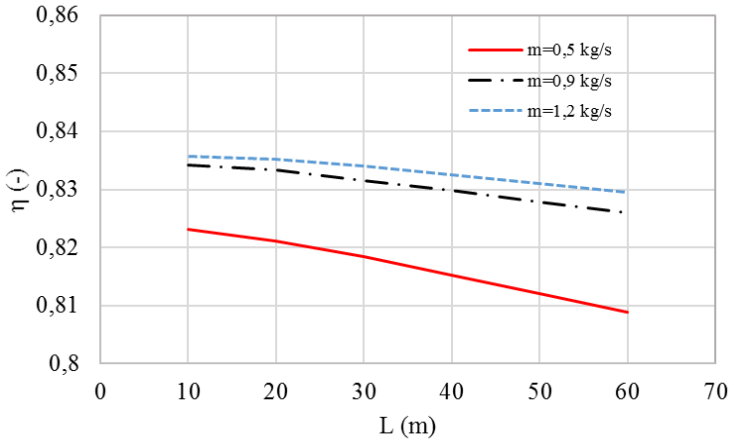


Figure 5. Thermal efficiency vs. length of the absorber tube for different fluid mass flow rates.

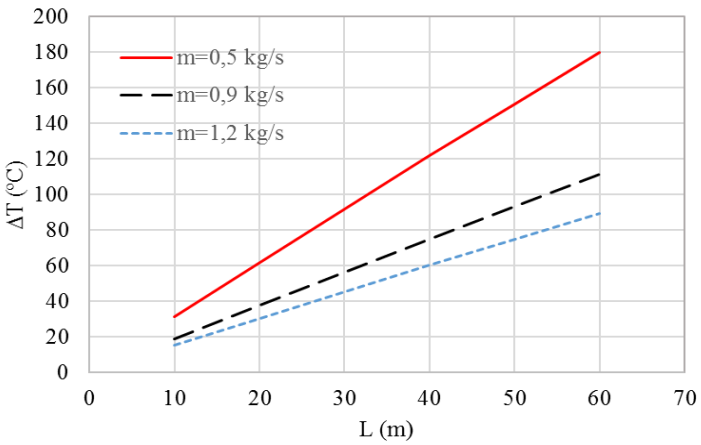


Figure 6. Fluid temperature variation vs. tube absorber length for different fluid mass flow rates.

It is possible to observe that increasing the mass flow rate, the efficiency increases because the fluid temperature difference decreases. The average fluid temperature diminishes and, consequently, the thermal losses.

Figure 7 shows that the thermal loss also increases with increasing the length of tube and the incident DNI value.

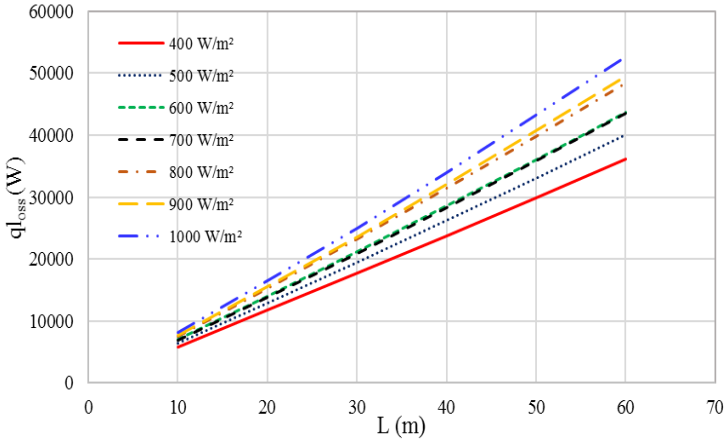


Figure 7. Heat loss vs. length of the absorber tube for different DNI.

Figure 8 shows the relation between the thermal efficiency and the temperature of the absorber for different DNI values. According to the increase of the temperature of the absorber, the thermal performance decreases. This is in accordance with what has been described in Figure 5: with increasing tube length decreases the thermal efficiency as a function of increasing temperature variation. In addition, still in Figure 8, it turns out that the performance increases as DNI is higher. Therefore, for times of the year when DNI is higher, better will be the performance of the system. The efficiency for higher DNI values and lower absorber temperatures tends to be constant, increasing the difference as the temperature increases. This result agrees with that showed by Hoffer *et al.* (2015).

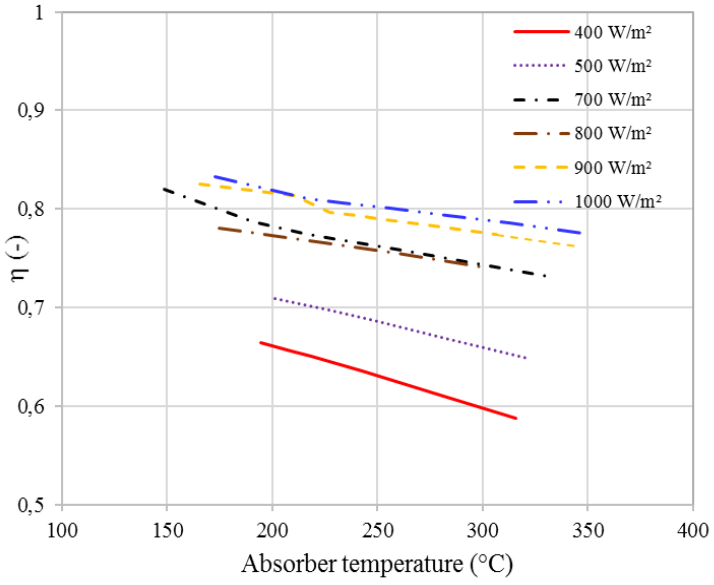


Figure 8. Thermal efficiency vs. absorber temperature for different incident DNI.

The performance can still be analyzed according to the properties of the absorber tube. In this paper, the effects of emissivity (Figure 9) were analyzed for different mass flow rates. As can be expected, lower emissivity in the infrared wavelength imply in lower thermal losses, increasing the thermal efficiency.

It is possible to observe that the thermal losses increase with the increasing of the emissivity and with the decreasing in mass flow rate, consequently the efficiency decreases. For example, for the flow rate of 0.54 kg/s the thermal loss increases 98,20 % and the efficiency decreases 99,50 % as the emissivity increased from 0.1 to 0.4.

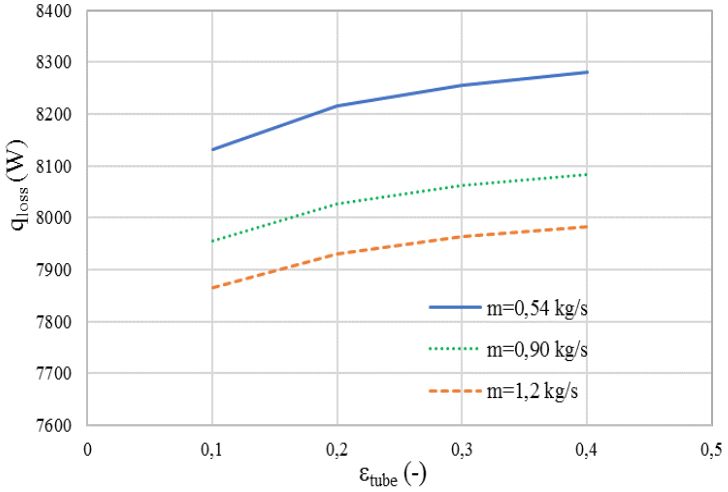


Figure 9. Thermal loss vs. absorber tube emissivity.

## 5. CONCLUSION

The objective of this work was to study a LFR system as a way of replacing nonrenewable sources of energy for heat production. For that, geometric and thermal aspects that can influence the performance of an LFR arrangement were analyzed. The focus of this work was the detailed study of the performance of the absorber element and its analysis was divided into two stages: (1) optical analysis and; (2) thermal analysis.

For optical analysis, the ray tracing was done to verify the behavior of the rays in a secondary concentrator of the type CPC. It was found that for the use of only one tube within the receiving cavity the intercept factor of 57%.

Another point analyzed, was the thermal behavior of the system, since the radiation incident on the receiver is converted into heat to feed industrial processes. The receiver used for the thermal analysis was the CPC, with an absorber tube positioned in the center of the parabolas (9 cm high in relation to the base of the receiver) of diameter 50 mm. To maximize the thermal effects of the system, a glass plate was inserted, and the secondary concentrator was isolated. For this study, Therminol VP1 fluid was used, which, as can be observed, meets the demands of the system, causing the amount of radiation converted to heat to be high.

Using this configuration for the receiver - secondary concentrator CPC format with aperture of 350 mm and one tube positioned 90 mm from the base of the receiver - the average efficiency values found were for the best analyzed - incident DNI of 1000 W/m² - reaches 80% and for the worse condition - DNI of 400 W/m² - the average efficiency is 65%. It is observed that the longer the length of the absorber tube, higher will be fluid temperature variation between the inlet and the outlet. In addition, the larger the mass flow rate of the fluid, the shorter the thermal exchange time of the same. These factors cause losses, which influence the performance of the system.

In this way, it is possible to observe that for the present study, linear Fresnel concentrators, besides presenting a satisfactory optical performance, have a high efficiency, even for times of the year in which the radiation incidence is lower.

## 6. ACKNOWLEDGEMENTS

This work is supported by CNPq/Brazil, contract 406976/2013-9, Chamada: Linha 2 - Energia Heliotérmica.

## 7. REFERENCES

Abbas, R., Muñoz, J., and Martínez-Val, J. M., 2012. "Steady-state thermal analysis of an innovative receiver for linear Fresnel reflectors". *Applied Energy*, Vol. 92, p. 503-515.

Balaji, S., Reddy, K. S. and Sundararajan, T., 2016. "Optical modelling and performance analysis of a solar LFR receiver system with parabolic and involute secondary reflectors". *Applied Energy*, Vol. 179, p. 1138-1151.

Heimsath, A., Cuevas, F., Hofer, A., Nitz, P. and Platzer, W. J., 2014. "Linear Fresnel collector receiver: heat loss and temperatures". *Energy Procedia*, Vol. 49, p. 386-397.

Hoffer, A., Cuevas, F. Heimsath, A. Nitz, P. Platzer, W. J. and Scholl, S. (2015) "Extended heat loss and temperatures analysis of three linear Fresnel receiver designs". *Energy Procedia*, Vol. 69, p. 424-433.

Lai, Y., Wu, T., Che, Sh., Dong, Z., Lyu, M., 2013. "Thermal performance prediction of a trapezoidal cavity absorber for a linear Fresnel Reflector". *Advances in Mechanical Engineering*, Vol. 2013, p. 7.

Modest, M. F., 2003. "Radiative heat transfer". 2 ed. *Burlington*: Academic Press.

Moghimi, M. A., Craig K. J. and Meyer, J. P., 2015. "Optimization of a trapezoidal cavity absorber for the Linear Fresnel Reflector". *Solar Energy*. Vol. 119, p. 343-361.

Muller, J. C., 2016. "Estudo geométrico de um refletor Fresnel linear para produção de energia térmica". Master Dissertation, Universidade do Vale do Rio dos Sinos, São Leopoldo.

Natarajan, S. K., Reddy K. S. and Mallick, T. K., 2012. "Heat loss characteristics of trapezoidal cavity receiver for solar linear concentrating system". *Applied Energy*, Vol. 93, p. 523-531.

Qiu, Y.; He, Y.; Cheng, Z.; Wang, K., 2015. "Study on optical and thermal performance of a linear Fresnel reflector using molten salt as HTF with MCRT and FVM methods". *Applied Energy*, Vol. 146, p. 162-173.

Sahoo, S. S.; Singh, S. and Banerjee, R., 2012. "Analysis of heat losses from a trapezoidal cavity used for a Linear Fresnel Reflector system". *Solar Energy*, Vol. 86, p. 1313 – 1322.

Walker, G. S., 2013. "Development of a low cost linear Fresnel solar concentrator". Master Dissertation, University of Stellenbosch, Stellenbosch.

Wong, R. L., 1976. "User's manual for CNVUFAC the General Dynamics heat transfer radiation view factor program". *California*: Lawrence Livermore National Laboratory Technical report.

## 8. RESPONSIBILITY NOTICE

The authors are the only responsible for the printed material included in this paper.